 Nucleic Acids Research, 1999, Vol. 27, No. 24 **4679–4686**

Geometry of a complex formed by double strand break repair proteins at a single DNA end: recruitment of DNA-PKcs induces inward translocation of Ku protein

Sunghan Yoo and William S. Dynan*

Program in Gene Regulation, Institute of Molecular Medicine and Genetics, Medical College of Georgia, 1120 15th Street, Augusta, GA 30912, USA

Received September 13, 1999; Revised and Accepted October 25, 1999

ABSTRACT

Ku protein and the DNA-dependent protein kinase catalytic subunit (DNA-PKcs) are essential components of the double-strand break repair machinery in higher eukaryotic cells. Ku protein binds to broken DNA ends and recruits DNA-PKcs to form an enzymatically active complex. To characterize the arrangement of proteins in this complex, we developed a set of photocross-linking probes, each with a single free end. We have previously used this approach to characterize the contacts in an initial Ku–DNA complex, and we have now applied the same technology to define the events that occur when Ku recruits DNA-PKcs. The new probes allow the binding of one molecule of Ku protein and one molecule of DNA-PKcs in a defined position and orientation. Photocross-linking reveals that DNA-PKcs makes direct contact with the DNA termini, occupying an ~10 bp region proximal to the free end. Characterization of the Ku protein cross-linking pattern in the presence and absence of DNA-PKcs suggests that Ku binds to form an initial complex at the DNA ends, and that recruitment of DNA-PKcs induces an inward translocation of this Ku molecule by about one helical turn. The presence of ATP had no effect on protein–DNA contacts, suggesting that neither DNA-PK-mediated phosphorylation nor a putative Ku helicase activity plays a role in modulating protein conformation under the conditions tested.

INTRODUCTION

DNA double-strand breaks (DSBs) are the critical lesions induced by ionizing radiation. In higher eukaryotes, most DSB repair occurs via a direct end-joining pathway. This pathway requires the heterodimeric Ku protein and at least six other polypeptides. Ku forms the initial complex with broken DNA ends. Ku binds avidly to all types of DNA ends *in vitro*, independent of their exact structure and sequence (reviewed in 1). Ku recruits the DNA-dependent protein kinase catalytic subunit (DNA-PKcs) to the DNA end, forming a complex that has protein kinase activity (2,3). This complex evidently forms the framework for recruitment of additional repair proteins, which include a ligase (DNA ligase IV), a nuclease (MRE 11), and a number of proteins that function as structural components of the repair machine (XRCC4, RAD50, p95/NBS1) (reviewed in 4–6).

The present studies focus on defining the events that occur when DNA-PKcs is recruited to the Ku–DNA complex. DNA-PKcs, which is a 470 kDa polypeptide, is a member of the phosphatidyl inositol 3-kinase family (7,8). The kinase activity of DNA-PKcs is essential for DSB repair *in vivo* and *in vitro* (9–13). Kinetic analysis in a cell-free repair system suggests that DNA-PKcs phosphorylates a critical local target within the repair complex (14). This target has not been identified, but could be an amino acid residue in XRCC4, Ku protein or DNA-PKcs itself (15–19).

Early studies showed that DNA-PKcs directly contacts DNA, as evidenced by UV photocross-linking (3) and by the ability of DNA to activate DNA-PKcs in the absence of Ku protein, under some experimental conditions (20). Subsequent work using high concentrations of DNA-PKcs showed that it can form a stable complex with DNA in the absence of Ku (21,22). Low-resolution structural studies reveal channels in DNA-PKcs that are potentially able to accommodate double-stranded DNA (23,24). Despite the evidence for direct contact with DNA, DNA-PKcs does not produce a clear footprint in DNase protection assays, and the size and boundaries of the DNA binding site are therefore not well-defined. Curiously, formation of the DNA-PKcs-containing complex is subject to the same stringent geometric constraints as with the Ku–DNA-complex itself, that is, complex formation is dependent on the presence of a free DNA end (21,22). The finding that Ku and DNA-PKcs have an independent capability to recognize DNA ends suggests that both proteins come into contact with the DNA termini during repair. Whether this contact is simultaneous or sequential is unknown.

To investigate the geometry of repair complexes containing Ku and DNA-PKcs, we developed a photocross-linking approach based on short oligonucleotide probes. One end of

*To whom correspondence should be addressed. Tel: +1 706 721 8756; Fax: +1 706 721 8752; Email: dynan@immag.mcg.edu
Present address:
Sunghan Yoo, Department of Radiation Medicine, Georgetown University Medical Center, 3970 Reservoir Road NW, Washington, DC 20007-2197, USA

the DNA is blocked, forcing the other end to become the sole locus of repair complex assembly. The resulting complexes have a unique orientation on the DNA, allowing the determination of which subunits of the repair complex are in contact with specific areas of the DNA surface. We have used this approach to describe Ku–DNA contacts in an initial complex formed with a 14mer oligonucleotide (25). The DNA binding domain of the 70 kDa Ku subunit (Ku70) occupies a pocket in the major groove proximal to the free end, whereas the 80 kDa Ku subunit (Ku80) probably contacts a region of the adjacent minor groove, distal to the DNA end.

We now show that DNA-PKcs, when bound in a complex containing Ku and DNA, makes direct contact with an ~10 bp region encompassing the DNA termini. Recruitment of DNA-PKcs to the initial Ku–DNA complex induces an inward translocation of Ku by about one helical turn. Although DNA-PKcs has autophosphorylation activity and Ku reportedly has intrinsic helicase activity, we found no evidence for ATP-dependent remodeling of complexes containing Ku and DNA-PKcs.

MATERIALS AND METHODS

Protein purification

DNA-PKcs was purified from HeLa cell nuclear extracts as described previously (20), except that the phenyl-Superose and Mono S steps were omitted. Non-histidine-tagged recombinant Ku protein was produced by coinfection of Sf9 cells with VBB2-86Ku and VBB2-70Ku (25,26) and was purified by Superdex 200, single-stranded DNA agarose and heparin-agarose chromatography as described (25).

DNA probes

The DNA probes used in this study are diagrammed in Figure 1. Aryl azide groups were introduced by reaction of azidophenacyl bromide with phosphorothioate-modified DNA as described (25), and iodopyrimidines were introduced by chemical synthesis. Probes with photocross-linkable groups on the top strand were radiolabeled at the 5′ end of the top strand using [γ-^{32}P]ATP and T4 polynucleotide kinase, and probes with photocross-linkable groups on the bottom strand were radiolabeled at the 3′ end of the bottom strand by a fill-in reaction using [α-^{32}P]dGTP and reverse transcriptase, as described (25).

Electrophoretic mobility shift assays

Assays were performed using radiolabeled 28mer probes as shown in Figure 1, or using double-stranded 24mer and 32mer DNAs containing the following top strand sequences: d(CTCAGGCGTTGACGACAACCCCTC) and d(CTCAGGCGTTGACGACAACCCCTCGCCCGCCC). Binding reactions were initiated by incubating DNA (7–15 nM) and streptavidin (1 μM) (Sigma, St Louis, MO) at room temperature for 30 min in 25 mM Tris–HCl, pH 7.9, 0.5 mM EDTA, 10% glycerol and 5 mM $MgCl_2$. Ku (20 nM) and DNA-PKcs (20 nM) were added and allowed to incubate for 30 min. Aliquots were analyzed by 5% non-denaturing polyacrylamide gel electrophoresis (PAGE) in a buffer containing 25 mM Tris–HCl, pH 8.3, 190 mM glycine and 1 mM EDTA.

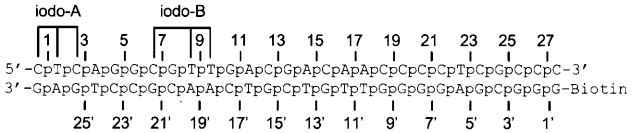

Figure 1. Sequence of DNA probes used in this study. Each of the aryl azide-modified 28mer probes contained an aryl azide modification at one of the positions indicated by the vertical lines and numbers. Iodopyrimidine-substituted 28mer DNAs had iodopyrimidine substitutions at two positions, as indicated (iodo-A and iodo-B). Biotin was incorporated as shown.

Photocross-linking

For aryl-azide based photocross-linking, protein–DNA complexes were formed in Eppendorf polyethylene microcentrifuge tubes that were placed inside a disposable polystyrene cell culture plate. The plates were irradiated with 302 nm ultraviolet light (AlphaImager 2000, Alpha Innotech, San Leandro, CA) for 25 s. Reactions were terminated by addition of SDS–PAGE sample buffer (62.5 mM Tris–HCl, pH 6.8, 5% glycerol, 2% SDS, 5% 2 mercaptoethanol, 1% bromphenol blue) and heated for 3 min at 100°C. Products were resolved by 7% SDS-PAGE and detected by PhosphorImager analysis. For iodopyrimidine-substituted photocross-linking, protein–DNA complexes were formed in Eppendorf polyethylene microcentrifuge tubes, and cross-linking was carried out in Eppendorf microcentrifuge tubes for 30 min using a 325 nm helium–cadmium laser (Omnichrome, Chino, CA).

Kinase assay

Kinase assays with a p53-derived peptide were performed as previously described (27). Various amounts of 28mer DNAs with and without biotin were incubated with 1 μM streptavidin (Sigma, St Louis, MO) in 25 mM Tris–HCl, pH 7.9, 25 mM $MgCl_2$, 1.5 mM DTT, 50 mM KCl and 10% glycerol at room temperature for 30 min. Reactions were further incubated at 30°C in the presence of 20 nM Ku protein, 18.5 nM DNA-PKcs, 70 μM peptide and 40 μM [γ-^{32}P]ATP (12.5 Ci/mmol) in a total volume of 20 μl. Reactions were stopped by addition of 10 μl of 1 mg/ml BSA and 10 μl of 40% TCA, and further incubated for 30 min on ice. Precipitated protein was removed by centrifugation and 10 μl of each supernatant was spotted on a phosphocellulose filter (Whatman P81). The filters were washed three times with 15% HOAc for 15 min, and incorporation of radiolabel was measured by liquid scintillation counting.

RESULTS

Formation of stable complexes containing Ku and DNA-PKcs

To avoid the ambiguity that would result if repair complexes were assembled in two different orientations, we used double-stranded DNA probes with a biotin group covalently attached at the 5′ end of one strand. Binding of streptavidin blocks one end, making the other end the site of assembly for repair complexes. We have previously used this strategy to analyze the initial Ku–DNA complex (25), and we now use the same strategy to analyze higher-order complexes containing Ku, DNA-PKcs and DNA.

Previous work has shown that the minimum length of DNA that permits the assembly of a stable, enzymatically active

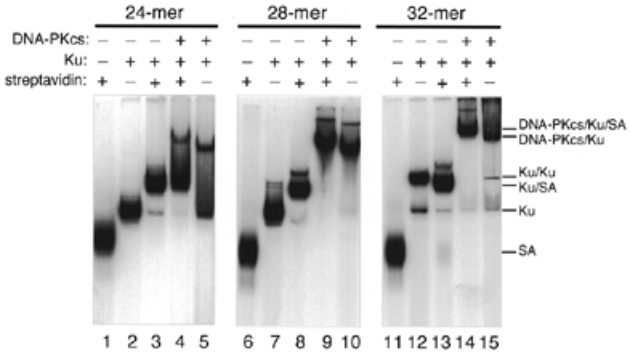

Figure 2. Electrophoretic mobility shift assays using 24mer, 28mer and 32mer probes. Binding reactions were performed as described in Materials and Methods using radiolabeled DNA (without aryl azide modifications). Radiolabeled complexes containing bound protein and DNA were visualized by PhosphorImager analysis. Positions of the complexes and the proteins that are present in each are indicated on the right. SA refers to streptavidin.

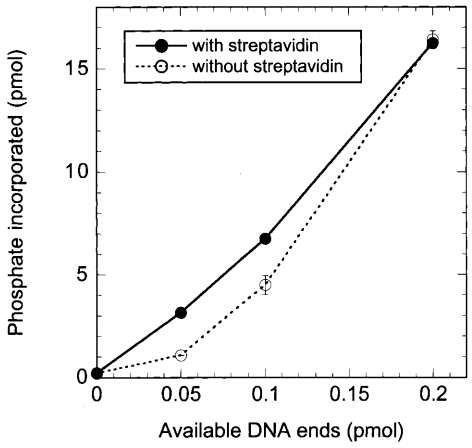

Figure 3. Complexes assembled on the 28mer DNA are enzymatically active. DNA-PKcs and Ku protein were allowed to bind to various amounts of 28mer DNA in the presence and absence of streptavidin, as indicated, and incorporation of radiolabeled phosphate into p53 peptide was measured as described in Materials and Methods. Background incorporation in the absence of enzyme has been subtracted.

Ku–DNA-PKcs complex is between 26 and 30 nt (28). It was necessary to confirm that oligonucleotides of this length were sufficient for complex assembly when one end was blocked with streptavidin. Results of a binding experiment using a 28mer oligonucleotide are shown in Figure 2. This DNA formed distinct, stable complexes with streptavidin (lane 6), with Ku (lane 7), with Ku and streptavidin (lane 8), and with Ku, DNA-PKcs and streptavidin (lane 9). Comparison of Ku–DNA-PKcs–DNA complexes assembled in the presence and absence of streptavidin shows that streptavidin alters the mobility of the complexes but not the efficiency of formation (compare lanes 9 and 10). Complexes formed on the 28mer DNA apparently contain only one Ku heterodimer, based on the absence of intermediate complexes in the reaction containing Ku and DNA alone (lane 7) and consistent with previous estimates of spacing requirements for Ku binding (reviewed in 1).

Binding assays were also performed with DNAs that were longer and shorter than the 28mer. A 24mer DNA formed stable complexes with streptavidin and Ku (lanes 1–3), but formation of DNA-PKcs-containing complexes was inefficient (lanes 4 and 5), as expected (25). A 32mer DNA formed stable DNA-PKcs-containing complexes (lanes 14 and 15), but unlike shorter DNAs, allowed binding of two Ku heterodimers in the reaction containing Ku and DNA alone (lane 12, indicated as Ku/Ku). Binding of more than one Ku potentially complicates interpretation of cross-linking results. Taken together, these data indicated that the 28mer was the optimal length for our experiments.

Complexes formed on single-ended 28mer are enzymatically active

To confirm that the Ku–DNA-PKcs complexes formed on the single-ended 28mer had protein kinase activity, we assembled complexes as in Figure 2 and performed a p53 peptide phosphorylation assay in the presence and absence of streptavidin. In Figure 3, phosphopeptide product has been plotted as a function of available DNA ends. We assumed that the 28mer had one available end in the presence of streptavidin or two in its absence. Enzymatically active complexes were formed with the 28mer oligonucleotide both in the presence and absence of streptavidin. Each complex apparently formed 50–80 molecules of phosphopeptide product in a 30 min reaction.

Streptavidin orients the binding

To determine whether blockage of one DNA end with streptavidin is effective as a means of orienting the Ku–DNA-PKcs complexes, we compared the photocross-linking pattern obtained in the presence and absence of streptavidin. We used probes with photocross-linkable aryl azide groups attached either near the free end (probe 3) or near the biotinylated end (probe 25) of the DNA, as diagrammed in Figure 4. Complexes were formed, subjected to UV irradiation, and cross-linked products were analyzed by SDS–PAGE.

The DNA-PKcs formed a prominent cross-linked adduct migrating in the region of >350 kDa (Fig. 4, upper panels, as marked). In the presence of streptavidin (lanes 1–3 and 7–9) there was a marked asymmetry in the DNA-PKcs cross-linking pattern. DNA-PKcs cross-linked selectively to probe 3, both in the presence and absence of Ku (lanes 2 and 3). DNA-PKcs cross-linked much less efficiently to probe 25 (lanes 8 and 9). The two Ku protein subunits also formed cross-linked adducts (lower panels). In the absence of DNA-PKcs, Ku70 cross-linked strongly to probe 3 and not to probe 25 (lanes 1 and 7). In the presence of DNA-PKcs, Ku70 cross-linking was much weaker but still showed some preference for probe 3 (lanes 2 and 8). Ku80 showed somewhat different behavior, cross-linking weakly, but preferentially, to probe 25 in the presence of DNA-PKcs (lane 8), and to probe 3 in the absence of DNA-PKcs (lane 1).

When streptavidin was omitted, the cross-linking pattern became much more symmetric. DNA-PKcs cross-linked strongly to both ends of the DNA (lanes 5, 6, 11 and 12). In the absence of DNA-PKcs, Ku70 cross-linked strongly to both ends and Ku80 cross-linked weakly to both ends (lanes 4 and 10). Overall, the results are consistent with the presence of

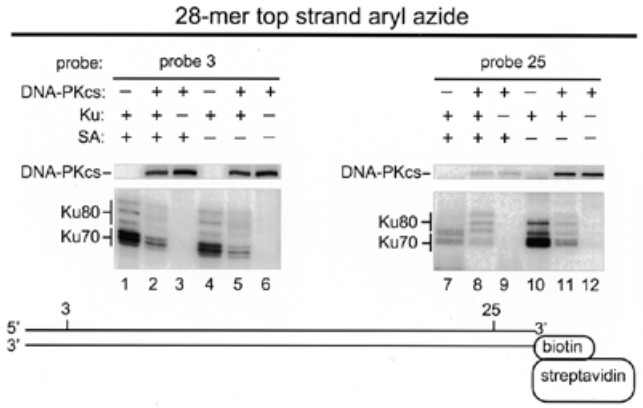

Figure 4. Effect of streptavidin on the cross-linking of Ku and DNA-PKcs to different aryl azide-derivatized 28mer probes. Cross-linking reactions were performed using radiolabeled probes with an aryl azide modification on the top strand at the positions indicated (probes 3 and 25). Relative positions of aryl azide modifications are indicated in a diagram below. Reactions were performed in the absence or in the presence of streptavidin (SA). Cross-linked products were analyzed by SDS–PAGE and visualized by PhosphorImager analysis. All panels are from the same experiment. Positions of DNA-PKcs, Ku70 and Ku80 adducts are indicated on the left. Multiple bands in the 70–80 kDa region apparently correspond to different conformational and geometric isomers. The identity of bands marked as Ku70 and Ku80 adducts was confirmed in separate experiments comparing wild type Ku and histidine-tagged Ku, as described (25).

oriented complexes in the presence of streptavidin and a mixture of complexes in two orientations in its absence.

Definition of Ku and DNA-PKcs contacts using a full set of 28mer aryl azide probes

To more fully define the geometry of the Ku–DNA-PKcs–DNA complex, as well as the changes in Ku–DNA contacts that occur when DNA-PKcs is recruited to the DNA, we performed cross-linking with a larger number of probes. We derivatized every second phosphate position on both strands of the DNA. Since each aryl azide group reacts with proteins within a 9 Å radius (29), this provides saturation coverage of the DNA surface. Probes 1–27 have aryl azide modifications on the top strand and probes 1′–25′ have modifications on the bottom strand (see Fig. 1, Materials and Methods). Unmodified control DNA was also prepared. Binding reactions were performed in the presence of Ku alone or Ku and DNA-PKcs together. All reactions contained streptavidin. Electrophoretic mobility shift analysis was performed, which showed that all probes formed quaternary complexes containing Ku, DNA-PKcs and streptavidin with similar efficiency (Fig. 5A and B).

Cross-linked products were analyzed by SDS–PAGE (Fig. 5C–H). Certain trends are apparent from inspection of the primary data. For example, DNA-PKcs cross-linked to a number of positions on both strands near the free end (Fig. 5C, probes 1–13, and D, probes 17′–25′). In the presence of DNA-PKcs, Ku70 cross-linked very strongly to certain positions on the top strand near the center of the DNA (Fig. 5E, probes 15–19) and to a more diffuse set of positions on the bottom strand (Fig. 5F). Ku80 cross-linked mostly to positions away from the free end (Fig. 5E, probes 15–27, and F, probes 1′–13′. In the absence of DNA-PKcs, there were a number of differences in the pattern of Ku–DNA contacts. Ku70 formed cross-links much more strongly to certain sites on the top strand near the free end (Fig. 5G, lanes 1–9), and the Ku80 contacts shifted toward the middle of the fragment (Fig. 5H).

Quantitation reveals a systematic shift in Ku–DNA contacts in the presence of DNA-PKcs

The relative amount of each cross-linked adduct was measured and plotted as a function of position of the cross-linker along

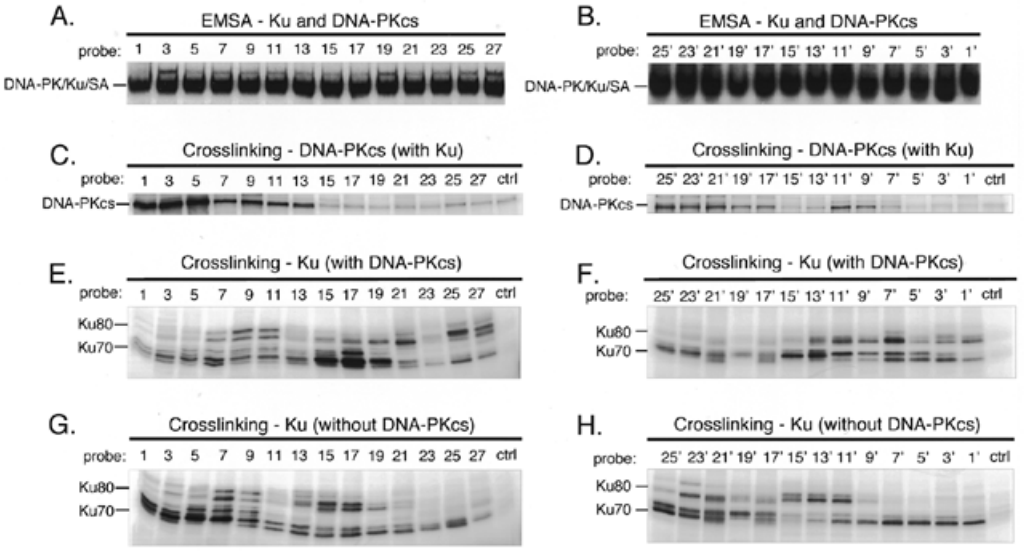

Figure 5. Cross-linking of Ku and DNA-PKcs to a full set of 28mer probes in the presence of streptavidin. (**A** and **B**) Binding reactions were carried out with top strand probes 1–27 (A) and bottom strand probes 1′–25′ (B). Reactions were analyzed by electrophoretic mobility shift assay to demonstrate formation of the quaternary complex containing streptavidin, Ku, DNA-PKcs and DNA. (**C**–**F**) Cross-linking reactions were performed using radiolabeled probes with an aryl azide modification on the top strand (probes 1–27) or bottom strand (probes 1′–25′) and products were analyzed by SDS–PAGE. (C and D) show upper portion of gel containing DNA-PKcs adducts. (E and F) show lower portion of same gel containing Ku70 and Ku80 adducts. (**G** and **H**) Same as (E) and (F) but reactions were performed in absence of DNA-PKcs.

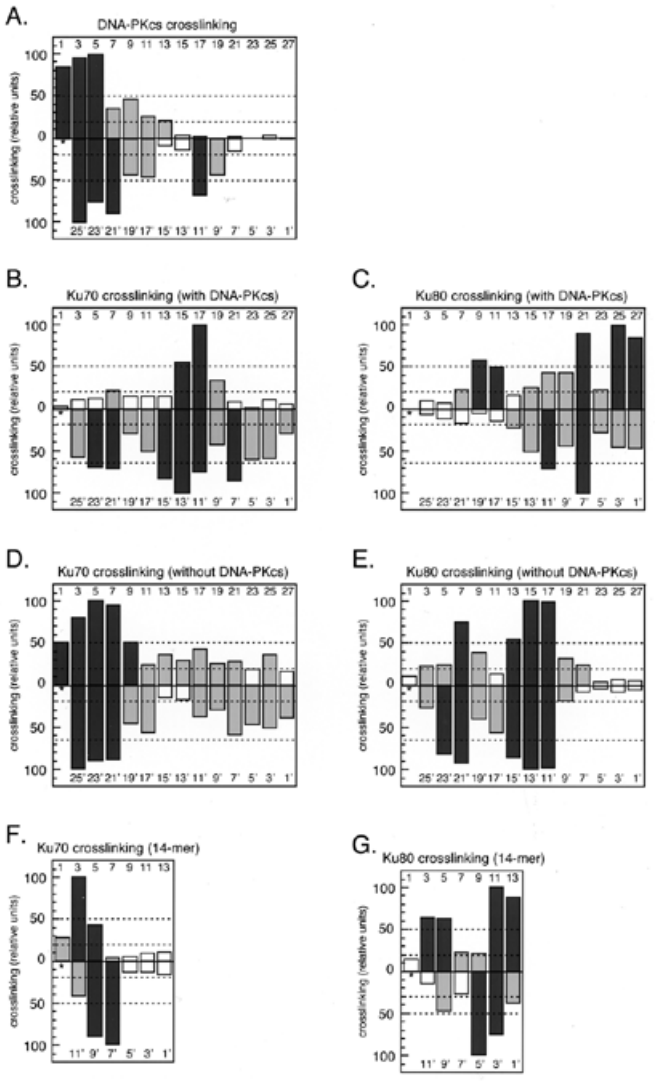

Figure 6. Quantitation of DNA-PKcs and Ku cross-linking data from Figure 5. For each subunit, the background in the absence of aryl azide modification was subtracted. Results were normalized and expressed as a percentage of the strongest cross-link on each strand. Cross-linking is plotted as a function of position of cross-linker attachment, with cross-linkers nearest the free end at the left and cross-linkers nearest the blocked end at the right. Bars extending above the horizontal axis denote relative cross-linking to top strand probes. Bars extending below the horizontal axis denote relative cross-linking to bottom strand probes. Dashed horizontal lines indicate threshold values for strong and moderately strong cross-linking (see text). Bars denoting strong and moderately strong crosslinking are shaded in dark and light gray, respectively, to facilitate visualize comparison of patterns seen in different panels. (**A**) Cross-linking of DNA-PKcs to 28mer probe in presence of Ku protein. (**B** and **C**) Cross-linking of Ku70 (B) and Ku80 (C) to 28mer probes in the presence of DNA-PKcs. (**D** and **E**) Cross-linking of Ku70 (D) and Ku80 (E) to 28mer probes in the absence of DNA-PKcs. (**F** and **G**) Cross-linking of Ku70 (F) and Ku80 (G) to 14mer DNA probe. Results in (F) and (G) are from a previous study (25) and are shown to facilitate comparison with cross-linking to the 28mer under similar conditions.

the DNA, starting from the free end (Fig. 6). Bars extending above and below the horizontal axis denote cross-linking to positions on the top and bottom strands of DNA, respectively. Within each panel, cross-linking has been normalized relative to the maximum value observed on each strand.

Cross-linking to DNA-PKcs is shown in Figure 6A. We classified the positions that cross-linked with relative efficiencies of 50–100% as strong protein–DNA contacts (dark shaded bars) and classified those that cross-linked with relative efficiencies of 20–49% as moderately strong protein–DNA contacts (light shaded bars). All other positions were classified as sites of non-contact (open bars). Although chosen arbitrarily, these thresholds are useful as an aid to interpretation. The strongest DNA-PKcs contacts are near the free end, with moderately strong contacts next to them. There are also a few significant DNA-PKcs contacts at positions near the center of the fragment.

The cross-linking of Ku subunits in the same reactions is shown in Figure 6B (for Ku70) and C (for Ku80). On the top strand, the same thresholds of 50 and 20% were used to classify strong and moderately strong contacts, respectively. On the bottom strand, a threshold of 65% was used to classify the strong contacts, to better differentiate them from the others. There is a cluster of strong Ku70 contacts on both strands near the center of the 28mer, with additional strong and weak contacts scattered more diffusely throughout the fragment. The Ku80 contacts are mostly in the distal half of the fragment, away from the free end, although there is also a cluster of contacts centered at position 9 on the top strand, overlapping the DNA-PKcs binding site.

The quantitation is particularly helpful in visualizing the difference in the location of the Ku subunits in the presence and absence of DNA-PKcs. Cross-linking of Ku protein in the absence of DNA-PKcs is shown in panels D and E. In the absence of DNA-PKcs, the strong Ku70 contacts are shifted away from the middle of the DNA, toward the free end, on both strands. A comparable shift in Ku80 contacts occurs, with a striking loss of contacts in the region distal to the free end, and a strengthening of the contacts both in the middle of the DNA and in the region proximal to the free end.

The pattern of Ku protein cross-linking in Figure 6D and E is remarkably similar to the results obtained in an earlier study characterizing the binding of Ku protein to a 14mer probe (25). To facilitate comparison, the results of the earlier work are summarized here in Figure 6F and G. With both the 14mer and the 28mer probes, Ku70 formed strong contacts on both strands of the DNA at positions near the free end. The peak region of contact is somewhat more compressed with the 14mer than with the 28mer, perhaps reflecting tight spatial constraints governing binding to the smaller probe. Ku80 formed two clusters of strong contacts. One cluster overlaps the Ku70 contacts in the region proximal to the free end; the other, which is unique to Ku80, is located more toward the interior of the fragment. The peak region of Ku80 contact is somewhat narrower with the 14mer than with the 28mer and is, in addition, shifted slightly toward the free end. Nevertheless, the resemblance between the 14mer and 28mer patterns is clear.

Major groove contacts defined using 28mer iodopyrimidine probes

To confirm that DNA-PKcs is in direct contact with the DNA termini, we tested two iodopyrimidine-substituted probes. Unlike aryl azide cross-linkers, which report the presence of proteins within ~9 Å of the probe attachment site, iodopyrimidine cross-linking is believed to require direct atomic contact between protein side chains and the C5 positions of cytidine

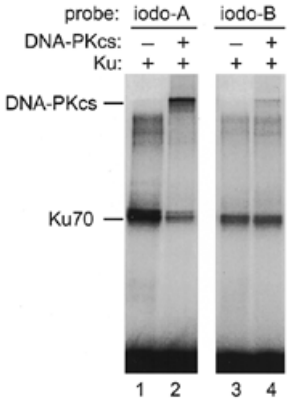

Figure 7. Cross-linking of Ku and DNA-PKcs to iodopyrimidine-substituted 28mer probes. Cross-linking reactions were performed using radiolabeled probes with iodopyrimidine substitutions on the top strand at the positions indicated (iodo-A and iodo-B, see Fig. 1). Reactions were performed in the presence of streptavidin. Cross-linked products were analyzed by SDS–PAGE and visualized by PhosphorImager analysis. Positions of Ku70 and DNA-PKcs adducts are indicated.

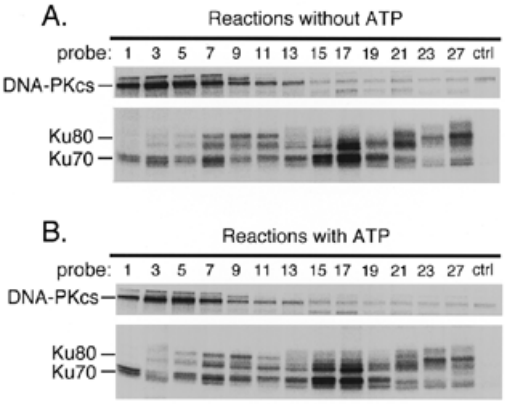

Figure 8. Cross-linking of Ku and DNA-PKcs in the presence or absence of ATP. Cross-linking reactions were performed using radiolabeled probes with an aryl azide modification on the top strand at the positions indicated (probes 1–23 and 27) in the absence of ATP (**A**) or in the presence of 1 mM ATP (**B**). Cross-linked products were analyzed by SDS–PAGE and visualized by PhosphorImager analysis. Positions of Ku70, Ku80 and DNA-PKcs adducts are indicated.

and thymidine, which lie in the major groove of duplex DNA (reviewed in 30). The iodopyrimidine cross-linking reaction is also somewhat chemically selective, favoring aromatic amino acids.

We prepared a probe with an iodopyrimidine substitution at the first three nucleotide positions on the top strand (probe iodo-A). In the absence of DNA-PKcs, this probe cross-linked almost exclusively to Ku70, as expected (Fig. 7, lane 1) (25). In the presence of DNA-PKcs, cross-linking to Ku70 was reduced and a distinctive DNA-PKcs adduct appeared (lane 2). These results are consistent with the model that DNA-PKcs is in direct contact with the DNA ends and significantly displaces the Ku protein. A probe with a triple iodopyrimidine substitution at nucleotides 7, 9 and 10 (probe iodo-B) showed less cross-linking to both Ku and DNA-PKcs (lanes 3 and 4). Although aryl azide probes revealed that DNA-PKcs is present in this general vicinity, it appears that there is limited direct contact between the iodo groups and appropriately reactive amino acids.

No evidence for ATP-dependent conformational changes in Ku or DNA-PKcs

It has been suggested that interaction of Ku and DNA-PKcs with DNA may be affected by ATP. Ku has been reported to have associated ATPase (31) and ATP-dependent helicase activities (32,33). Moreover, DNA-PKcs-mediated autophosphorylation apparently leads to inactivation of repair complexes and dissociation of DNA-PKcs from DNA (34). It was therefore of interest to determine whether ATP induced a significant change in the pattern of Ku and DNA-PKcs cross-linking.

Binding reactions were performed in the presence and absence of ATP, subjected to cross-linking, and analyzed by SDS–PAGE, with results shown in Figure 8. The patterns of cross-linking were virtually identical in the presence and absence of ATP. Very minor changes in the pattern (e.g. a slight difference in Ku70:Ku80 ratios with probe 11) were not observed in other experiments. There were also no changes in the pattern of cross-linking in reactions containing ATP and the DNA-PKcs inhibitor, wortmannin, or in reactions containing ATP and Ku alone (data not shown). These data provide no evidence for ATP-dependent conformational changes under the conditions tested.

DISCUSSION

Protein–DNA contacts can most readily be analyzed using probes containing a single binding site for the protein of interest. This approach has been widely applied for proteins that recognize specific sequences, but is more difficult to implement with proteins, such as repair enzymes, that lack intrinsic sequence specificity. In the present study, we have used specially designed probes, which are of the minimum size that permits complex formation and that have only one free end. This has allowed us to trap the DSB repair proteins, Ku and DNA-PKcs, in a unique position and orientation and has enabled us to generate a detailed map of the contacts between these proteins and a free DNA end.

A principal conclusion is that DNA-PKcs makes extensive contacts with both strands of the DNA in the vicinity of the termini. The present work provides the first high-resolution definition of the DNA-PKcs binding site within the active Ku–DNA-PKcs complex. DNA-PKcs seems to cap the free end, displacing Ku protein toward interior positions. The localization of DNA-PKcs at the DNA termini is consistent with recent kinetic studies showing that DNA-PKcs regulates the ability of Ku to associate and dissociate from DNA fragments *in vitro* (10), and with atomic force microscopy (AFM) images showing that isolated DNA-PKcs binds at DNA ends and does not translocate inward (21). Because of its location at the DNA end, DNA-PKcs occupies a position where it could, in principle, mediate key steps in DSB repair, including synapsis of non-homologous ends.

The sites that cross-link to DNA-PKcs have been projected onto a model of B-form DNA in Figure 9. The free end is at the top and the blocked end is at the bottom. Contacts (dark green,

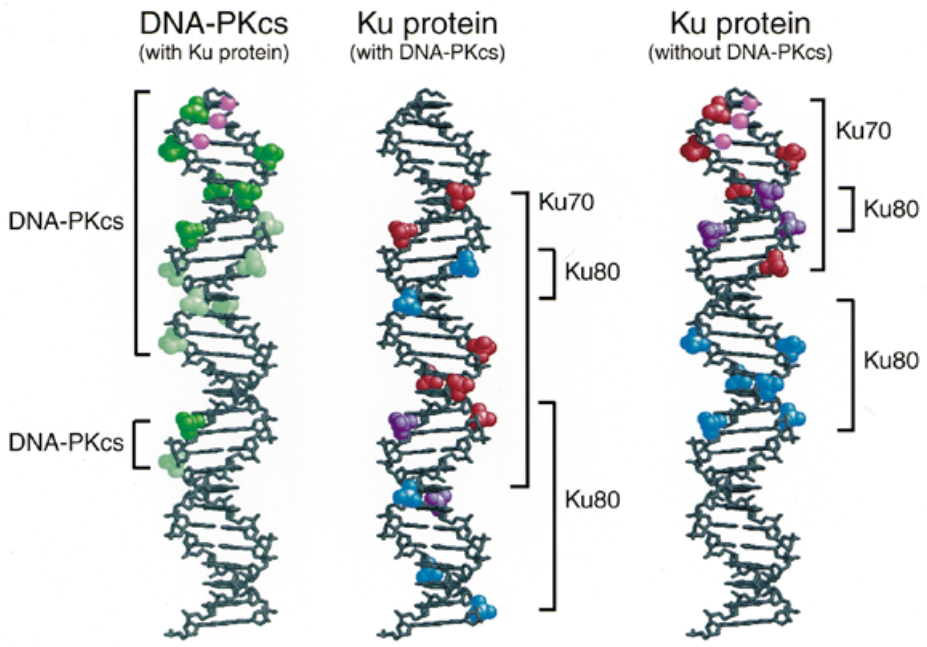

Figure 9. Three-dimensional representation of protein–DNA contacts. The 28mer sequence was modeled as B-form DNA, with free end at the top and blocked end at the bottom. Phosphate groups are highlighted to indicate positions of aryl azide cross-links. Dark green, strong DNA-PKcs contacts. Light green, moderately strong DNA-PKcs contacts. Red, strong Ku70 contacts. Blue, strong Ku80 contacts. Purple, strong contacts with both Ku70 and Ku80. Magenta, iodo groups present in probe iodo-A, which form strong contacts with DNA-PKcs or with Ku70 (in the absence of DNA-PKcs).

light green and magenta, see figure legend) are distributed around the circumference of the DNA. The contact region occupies about half the 28mer probe, but is small relative to the 470 kDa DNA-PKcs itself. Assuming that DNA-PKcs has a roughly spherical conformation, the binding site represents about one-third of the protein's diameter. This appears to rule out the idea that the DNA is extensively wrapped around the outside of DNA-PKcs, but is consistent with a proposed model where DNA ends penetrate within channels in the DNA-PKcs structure (23,35). The finding that the relatively bulky aryl azide groups did not affect the strength of protein–DNA interactions suggests that there is considerable flexibility in the protein–DNA interface. This may be important in allowing DNA-PKcs to bind to radiation-damaged DNA ends.

A second conclusion is that the recruitment of DNA-PKcs induces a concerted change in Ku protein–DNA contacts, consistent with an inward translocation of Ku by about one helical turn. Although it is known that Ku helps recruit DNA-PKcs to DNA, the effect of this recruitment on Ku–DNA contacts has not previously been established. Our data show that, when Ku binds initially to the 28mer, the majority of the molecules appear to remain bound near the free end. Contacts formed by Ku protein (without DNA-PKcs) have been projected onto B-form DNA in the rightmost model in Figure 9. As noted, there is a strong resemblance between the pattern of contacts in this complex and in the pattern formed with a 14mer in an earlier study (25). Because the 14mer is the smallest DNA that was capable of forming a stable Ku–DNA complex, we believe that cross-links between Ku and the 14mer represent a minimal set of contacts characteristic of the initial Ku–DNA recognition complex. When DNA-PKcs is recruited to DNA, these contacts appear to migrate inward, away from the free end.

Changes in Ku protein cross-linking are not absolute and, in particular, DNA-PKcs only partially suppressed Ku70 cross-linking at the positions near the free end. Morever, two sites of Ku80 contact (probes 9 and 11) were maintained in the proximal region even in the presence of DNA-PKcs. Possibly, these cross-links involve a sequence in Ku80 that contacts DNA-PKcs, which might be separate from the main Ku80 DNA binding domain. For example, it has been suggested that a peptide at the extreme C-terminus of Ku80 mediates DNA-PKcs contact (36,37).

A third conclusion is that ATP had no effect on the pattern of protein–DNA contacts. Some preparations of Ku protein have associated DNA-dependent ATPase and DNA helicase activity (31–33). The significance of these observations has been uncertain, as Ku lacks sequence similarity to other helicases, and mutation of a putative ATP binding motif in Ku80 had no effect on repair function (38,39). If Ku were active as an ATPase or helicase, one would predict that conformational changes in the presence of ATP would lead to an alteration in the pattern of protein–DNA contacts. The failure to observe such changes argues against the presence of an intrinsic ATP-dependent enzymatic activity within the Ku polypeptides under the conditions tested.

The DNA-dependent protein kinase has an autophosphorylation activity that has been linked to inactivation and dissociation of DNA-PKcs from DNA (34). DNA-PKcs also phosphorylates Ku protein at specific sites, several of which have been mapped (19,38). Although the 28mer was long enough to accommodate formation of an enzymatically active DNA–PK complex, there were no ATP-dependent changes in protein conformation that could be correlated with autophosphorylation activity. Recent work shows that a DNA-PKcs-mediated phosphorylation event regulates translocation of Ku

protein on longer DNA substrates (10). The single-ended 28mers may be too short for this phenomenon to be fully manifested. It also may be that only a fraction of the DNA-PKcs-containing complexes are enzymatically active, or, at the high concentrations of DNA-PKcs used in these experiments, new molecules of DNA-PKcs bind rapidly to replace molecules that dissociate after autophosphorylation.

Although the photocross-linking approach provides significant new information, it is subject to certain limitations. Importantly, the observed cross-linking pattern reflects the average position of the different polypeptides in the repair complex. In some instances, especially with Ku70 and probes derivatized on the bottom strand, the pattern of cross-linking was rather diffuse, with most probes showing some level of reactivity. This may reflect a broad distribution of contacts, or alternatively, a mixture of complexes containing Ku protein bound at different positions.

Another concern is that quaternary complexes might be unstable, with partial dissociation of DNA-PKcs occurring during the cross-linking reaction. To investigate this possibility, we performed two-dimensional experiments where proteins were first cross-linked to DNA, quaternary complexes were isolated on a native gel, and these complexes were analyzed in a second dimension by SDS–PAGE. This assured that only quaternary complexes were scored. Under these conditions, there was still appreciable cross-linking of Ku70 to positions near the free end (data not shown); suggesting that Ku70 retains some bona fide contacts near the DNA end even in the presence of DNA-PKcs.

We have not yet investigated the degree to which the binding of DNA-PKcs to the DNA end distorts the structure of DNA. Because non-homologous DNA end joining frequently occurs through regions of microhomology, it has been suggested that free ends may be unwound or resected by a nuclease in order to allow transient base pairing across opposite sides of the DNA break (1,40). Although we have modeled protein–DNA contacts onto B-form DNA, the actual conformation of the DNA may differ, particularly at the extreme termini or as the result of enzymatic processing that occurs during the repair reaction.

Genetic evidence implicates additional polypeptides in DSB repair, beyond those studied here. These polypeptides include DNA ligase IV, XRCC4 and the hMRE11/hRAD50/NBS1 complex (4–6). Photocross-linking, using single-ended oligonucleotides, should be applicable to characterization of protein–DNA contacts in higher-order complexes that include these proteins.

ACKNOWLEDGEMENTS

We thank N. Miller and F. Hudson for technical assistance and C. Hyde (National Institute of Child Health and Human Development) for coordinates of the 28mer DNA model. We thank R.-B. Markowitz for comments on the manuscript. This work was supported by a Biomedical Research Grant from the Arthritis Foundation.

REFERENCES

1. Dynan,W.S. and Yoo,S. (1998) *Nucleic Acids Res.*, **26**, 1551–1559.
2. Dvir,A., Peterson,S.R., Knuth,M.W., Lu,H. and Dynan,W.S. (1992) *Proc. Natl Acad. Sci. USA*, **89**, 11920–11924.
3. Gottlieb,T.M. and Jackson,S.P. (1993) *Cell*, **72**, 131–142.
4. Kanaar,R., Hoeijmakers,J.H. and van Gent,D.C. (1998) *Trends Cell Biol.*, **8**, 483–489.
5. Jeggo,P.A. (1998) *Radiat. Res.*, **150**, S80–S91.
6. Smith,G.C. and Jackson,S.P. (1999) *Genes Dev.*, **13**, 916–934.
7. Sipley,J.D., Menninger,J.C., Hartley,K.O., Ward,D.C., Jackson,S.P. and Anderson,C.W. (1995) *Proc. Natl Acad. Sci. USA*, **92**, 7515–7519.
8. Poltoratsky,V.P., Shi,X., York,J.D., Lieber,M.R. and Carter,T.H. (1995) *J. Immunol.*, **155**, 4529–4533.
9. Labhart,P. (1999) *Mol. Cell. Biol.*, **19**, 2585–2593.
10. Calsou,P., Frit,P., Humbert,O., Muller,C., Chen,D.J. and Salles,B. (1999) *J. Biol. Chem.*, **274**, 7848–7856.
11. Gu,X.Y., Bennett,R.A. and Povirk,L.F. (1996) *J. Biol. Chem.*, **271**, 19660–19663.
12. Baumann,P. and West,S.C. (1998) *Proc. Natl Acad. Sci. USA*, **95**, 14066–14070.
13. Izzard,R.A., Jackson,S.P. and Smith,G.C. (1999) *Cancer Res.*, **59**, 2581–2586.
14. Gu,X.Y., Weinfeld,M.A. and Povirk,L.F. (1998) *Biochemistry*, **37**, 9827–9835.
15. Chan,D.W. and Lees-Miller,S.P. (1996) *J. Biol. Chem.*, **271**, 8936–8941.
16. Critchlow,S.E., Bowater,R.P. and Jackson,S.P. (1997) *Curr. Biol.*, **7**, 588–598.
17. Leber,R., Wise,T.W., Mizuta,R. and Meek,K. (1998) *J. Biol. Chem.*, **273**, 1794–1801.
18. Modesti,M., Hesse,J.E. and Gellert,M. (1999) *EMBO J.*, **18**, 2008–2018.
19. Chan,D.W., Ye,R., Veillette,C.J. and Lees-Miller,S.P. (1999) *Biochemistry*, **38**, 1819–1828.
20. Dvir,A., Stein,L.Y., Calore,B.L. and Dynan,W.S. (1993) *J. Biol. Chem.*, **268**, 10440–10447.
21. Yaneva,M., Kowalewski,T. and Lieber,M.R. (1997) *EMBO J.*, **16**, 5098–5112.
22. Hammarsten,O. and Chu,G. (1998) *Proc. Natl Acad. Sci. USA*, **95**, 525–530.
23. Leuther,K.K., Hammarsten,O., Kornberg,R.D. and Chu,G. (1999) *EMBO J.*, **18**, 1114–1123.
24. Chiu,C.Y., Cary,R.B., Chen,D.J., Peterson,S.R. and Stewart,P.L. (1998) *J. Mol. Biol.*, **284**, 1075–1081.
25. Yoo,S., Kimzey,A. and Dynan,W.S. (1999) *J. Biol. Chem.*, **274**, 20034–20039.
26. Ono,M., Tucker,P.W. and Capra,J.D. (1994) *Nucleic Acids Res.*, **22**, 3918–3924.
27. Yoo,S. and Dynan,W.S. (1998) *Biochemistry*, **37**, 1336–1343.
28. West,R.B., Yaneva,M. and Lieber,M.R. (1998) *Mol. Cell. Biol.*, **18**, 5908–5920.
29. Burgin,A.B. and Pace,N.R. (1990) *EMBO J.*, **9**, 4111–4118.
30. Meisenheimer,K.M. and Koch,T.H. (1997) *Crit. Rev. Biochem. Mol. Biol.*, **32**, 101–140.
31. Cao,Q.P., Pitt,S., Leszyk,J. and Baril,E.F. (1994) *Biochemistry*, **33**, 8548–8557.
32. Ochem,A.E., Skopac,D., Costa,M., Rabilloud,T., Vuillard,L., Simoncsits,A., Giacca,M. and Falaschi,A. (1997) *J. Biol. Chem.*, **272**, 29919–29926.
33. Tuteja,N., Tuteja,R., Ochem,A., Taneja,P., Huang,N.W., Simoncsits,A., Susic,S., Rahman,K., Marusic,L., Chen,J. *et al.* (1994) *EMBO J.*, **13**, 4991–5001.
34. Chan,D.W. and Lees-Miller,S.P. (1996) *J. Biol. Chem.*, **271**, 8936–8941.
35. Chiu,C.Y., Cary,R.B., Chen,D.J., Peterson,S.R. and Stewart,P.L. (1998) *J. Mol. Biol.*, **284**, 1075–1081.
36. Singleton,B.K., Torres-Arzayus,M.I., Rottinghaus,S.T., Taccioli,G.E. and Jeggo,P.A. (1999) *Mol. Cell. Biol.*, **19**, 3267–3277.
37. Gell,D. and Jackson,S.P. (1999) *Nucleic Acids Res.*, **27**, 3494–3502.
38. Jin,S. and Weaver,D.T. (1997) *EMBO J.*, **16**, 6874–6885.
39. Singleton,B.K., Priestley,A., Steingrimsdottir,H., Gell,D., Blunt,T., Jackson,S.P., Lehmann,A.R. and Jeggo,P.A. (1997) *Mol. Cell. Biol.*, **17**, 1264–1273.
40. Chu,G. (1997) *J. Biol. Chem.*, **272**, 24097–24100.